Structural Engineering and Mechanics, *Vol. 60, No. 3 (2016) 455-470*
DOI: http://dx.doi.org/10.12989/sem.2016.60.3.455

Closed-form solutions for non-uniform axially loaded Rayleigh cantilever beams

Korak Sarkar[*1], Ranjan Ganguli[1] and Isaac Elishakoff[2]

[1]Department of Aerospace Engineering, Indian Institute of Science, Bangalore-560012, India
[2]Department of Mechanical Engineering, Florida Atlantic University, Boca Raton, FL 33431-0991, USA

(Received August 24, 2015, Revised August 10, 2016, Accepted September 6, 2016)

Abstract. In this paper, we investigate the free vibration of axially loaded non-uniform Rayleigh cantilever beams. The Rayleigh beams account for the rotary inertia effect which is ignored in Euler-Bernoulli beam theory. Using an inverse problem approach we show, that for certain polynomial variations of the mass per unit length and the flexural stiffness, there exists a fundamental closed form solution to the fourth order governing differential equation for Rayleigh beams. The derived property variation can serve as test functions for numerical methods. For the rotating beam case, the results have been compared with those derived using the Euler-Bernoulli beam theory.

Keywords: Rayleigh beam; free vibration; inverse problem; closed-form solution; test functions

1. Introduction

Elastic beams are used as a mathematical model for a wide variety of engineering structures like bridges, buildings, rotor blades, pillars, propeller blades, turbine blades etc. For long and slender beams, the Euler-Bernoulli beam theory is used as the basic model, which ignores the effects of rotary inertia and shear deformation (Abedinnasab, Zohoor *et al*. 2012, Bağdatlı and Uslu 2015, Baghani, Mohammadi *et al*. 2014, Liu, Yin *et al*. 2013, Maiz, Bambill *et al*. 2007, Mao, 2015, Sarkar and Ganguli 2013, 2014b, 2014c, Shahba, Attarnejad *et al*. 2011, Zahrai, Mortezagholi *et al*. 2016). On the other hand, the short and thick beams are typically modeled using the Timoshenko beam theory, which takes into account both the effects of rotary inertia and shear deformation (Aydin 2013, Bambill, Rossit *et al*. 2013, Calim, 2016, Datta and Ganguli 1990, Ebrahimi and Jafari 2016, Ke, Yang *et al*. 2009, Lou, Dai *et al*. 2006, Ma'en and Butcher 2012, Sarkar and Ganguli 2014a, Shahba, Attarnejad *et al.* 2011, Tang, Wu *et al*. 2014, Yesilce 2015). A relatively less known but simpler theory was developed by Lord Rayleigh before the Timoshenko beam theory came into existence. It includes the rotary inertia effect but does not take into account the shear deformation effect (Banerjee and Jackson 2013, Li, Tang *et al*. 2013, Xi, Li *et al*. 2013). Hence, application wise it is simpler than the Timoshenko beam theory as it leads to a single fourth order governing differential equation in a single variable as opposed to the coupled differential

∗Corresponding author, Research Student, E-mail: korakpom@gmail.com, koraksarkar@aero.iisc.ernet.in

http://www.techno-press.org/?journal=sem&subpage=8 ISSN: 1225-4568 (Print), 1598-6217 (Online)

equations in two variables for the latter case. The Rayleigh beam theory also predicts the natural frequencies and mode shapes more accurately than the Euler-Bernoulli beam theory, without going into the mathematical complexities of the Timoshenko beam theory. This work is motivated by the following observation. For varying axial loads (for example, gravity-loaded beam and rotating beam) the fourth order differential equation does not have any closed-form solution even for the case of uniform beam. Thus, it appears instructive to study axially loaded beam via Rayleigh theory. Researchers resort to various numerical or approximate methods when studying vibration problems related to Rayleigh beam theory (Chang, Lin *et al*. 2010, Pai, Qian *et al*. 2013, Stojanović and Kozić 2012).

Following previous works appear to be relevant. (Xi, Li *et al.* 2013) studied the free vibration of standing and hanging gravity-loaded Rayleigh cantilever beams. The authors reduced the problem to an integral equation and by seeking a non-trivial solution of the integral equation, a characteristic equation of free bending vibration of a gravity-loaded cantilever was derived approximately. Consequently, the natural frequencies and mode shapes were calculated. Using this method, (Li, Tang *et al.* 2013) also studied the transverse vibration of a Rayleigh cantilever beam with arbitrarily distributed axial loading and carrying a concentrated mass at the free end. (Banerjee and Jackson 2013) investigated the free vibration of rotating tapered Rayleigh beam using the dynamic stiffness method of solution. The authors illustrated the natural frequencies and mode shapes of some example beams, having cantilevered boundary condition, using the developed dynamic stiffness matrix and applying the Wittrick-Williams algorithm. (Auciello and Lippiello 2013) studied the vibration analysis of rotating non-uniform tapered Rayleigh beams using the “Cell Discretization Method” (CDM). Applying the dynamic variational approach, the equation of motion is derived by means of the Lagrange formulation for the multiple degree of freedom systems (MDOF). Recently, (Tang, Li *et al*. 2015) determined the natural frequencies for flapwise bending vibration of rotating tapered Rayleigh cantilever beams, using the integral equation method.

The literature on axially loaded Rayleigh beams clearly shows a need for closed form solutions which can be used to check and guide numerical approaches. A forward solution approach to solving the governing differential equation for non-uniform Rayleigh beams does not yield a closed-form solution, to the best of the authors’ knowledge. However, a semi-inverse problem approach of assuming a solution and then looking for the corresponding structure can yield a closed form solution. In this paper, we have extended Elishakoff's method (Elishakoff 2004, Elishakoff and Guede 2004, Sarkar 2012) for the case of an axially loaded non-uniform Rayleigh cantilever beam. We have shown that for certain mass per unit length distributions and flexural stiffness variations there exists a fundamental closed form solution of the governing differential equation. The obtained results can serve as benchmark solutions for various numerical methods and also provide valuable insights into the design of such beams if they are required to vibrate at or away from a pre-specified frequency range.

2. Mathematical formulation

We consider a non-uniform Rayleigh beam which is acted upon by a variable axial load $T(x)$. Considering harmonic vibration, the dynamics of this beam is governed by the fourth order differential equation given by (Banerjee and Jackson 2013, Li, Tang *et al.* 2013, Xi, Li *et al.* 2013)

Table 1 Commonly encountered axial loading $T(x)$ and their corresponding expressions for the frequency parameter κ in Rayleigh beam theory

Axial loading type	Expression for $\boldsymbol{T(x)}$	Expression for $\boldsymbol{\kappa}$
No axial load	$T(x) = 0$	$\kappa = \omega^2$
Uniform axial load	$T(x) = P$	$\kappa = \omega^2$
Gravity-loaded	$T(x) = \int_x^L \rho A(x) g\, dx$	$\kappa = \omega^2$
Centrifugally-loaded	$T(x) = \int_x^L \rho A(x) \Omega^2 x\, dx$	$\kappa = \omega^2 + \Omega^2$

$$\frac{d^2}{dx^2}\left[EI(x)\frac{d^2\phi(x)}{dx^2}\right] - \frac{d}{dx}\left[T(x)\frac{d\phi(x)}{dx}\right] - \rho A(x)\omega^2\phi(x) + \frac{d}{dx}\left[\rho I(x)\kappa\frac{d\phi(x)}{dx}\right] = 0 \quad (1)$$

where E is the elastic modulus, ρ is the material density, $I(x)$ is the area moment of inertia, $A(x)$ is the cross-sectional area, $\phi(x)$ is the mode shape, ω is the frequency, L is the length of the beam and κ is a frequency parameter depending on the type of loading. The expressions for different types of commonly encountered axial loads $T(x)$ and their corresponding expressions for κ are given in Table 1, where P is the uniform axial load, g is the acceleration due to gravity and Ω is the uniform rotation speed for the rotating beam. The first three terms on the LHS of Eq. (1) are also present in the Euler-Bernoulli beam equation (Gunda and Ganguli 2008). The fourth term is new for the Rayleigh beam and models the rotary inertia effect.

Eq. (1) does not have any closed-form solutions for non-uniform beams. For the gravity-loaded and centrifugally loaded case, Eq. (1) does not yield a closed-form solution even for a uniform beam. Therefore, we take a semi-inverse approach to solve Eq. (1). We assume the cross-sectional area variation $A(x)$ and the area moment of inertia $I(x)$ as simple polynomial functions given by

$$A(x) = a_0 + a_1x + a_2x^2 \quad (2)$$

$$I(x) = b_0 + b_1x + b_2x^2 + b_3x^3 + b_4x^4 \quad (3)$$

Note that the mass density ρ and elastic modulus E are assumed as constants. We investigate the class of special problems where the mode shape $\phi(x)$ will be represented by a simple polynomial satisfying all the necessary boundary conditions. The boundary conditions for a non-uniform Rayleigh cantilever beam, for different types of axial loading (Banerjee and Jackson 2013, Li, Tang *et al.* 2013, Xi, Li *et al.* 2013), are given in Table 2, where $\alpha = \rho/E$. The assumed mode shape $\phi(x)$ is sought as a fourth order polynomial function given by

$$\phi(x) = c_0 + c_1x + c_2x^2 + c_3x^3 + c_4x^4 \quad (4)$$

where c_i's are arbitrary constants which can be determined using the boundary conditions, given in Table 2, along with the condition of normalization given by $\phi(L) = 1$. The expressions for the constants c_i's for the uniform axially loaded beam and the gravity-loaded beam are given in Appendix A, Eq. (A.1), and for the rotating beam is given in Appendix A, Eq. (A.2). Since the boundary conditions for the beam under uniform axial load and gravity load are the same, hence their corresponding expressions for the constants c_i's are also the same. Once the expressions for the constants c_i's are determined for the different types of axial loading we can determine the

Table 2 Boundary conditions for a non-uniform Rayleigh cantilever beam for different types of axial loading

Axial loading type	Displacement at $\boldsymbol{x=0}$	Rotation at $\boldsymbol{x=0}$	Moment at $\boldsymbol{x=L}$	Shear at x = L
No axial load	$\phi(x)=0$	$\phi'(x)=0$	$\phi''(x)=0$	$\phi'''(x)+\alpha\omega^2\phi'(x)=0$
Uniform axial load	$\phi(x)=0$	$\phi'(x)=0$	$\phi''(x)=0$	$\phi'''(x)+\alpha\omega^2\phi'(x)=0$
Gravity-loaded	$\phi(x)=0$	$\phi'(x)=0$	$\phi''(x)=0$	$\phi'''(x)+\alpha\omega^2\phi'(x)=0$
Centrifugally-loaded	$\phi(x)=0$	$\phi'(x)=0$	$\phi''(x)=0$	$\phi'''(x)+\alpha(\Omega^2+\omega^2)\phi'(x)=0$

assumed mode shape $\phi(x)$, using Eq. (4).

Now, if we substitute the polynomial expressions for the $A(x)$ and $I(x)$ (given by Eqs. (2) and (3)), along with the assumed mode shape $\phi(x)$ (given by Eq. (4)), into the governing differential equation (given by Eq. (1)), we will get a polynomial equation in x of order six. If this polynomial equation has to be satisfied for all values of x $(0 \le x \le L)$ then the coefficient of the various powers of x must be set to zero, thus leading to seven linear equations in eight variables given by

$$[\mathbf{A}]\{\mathbf{y}\}=\{\mathbf{v}\} \tag{5}$$

where $\mathbf{A}$ is a 7x8 matrix, $\mathbf{y}=\{a_0,a_1,a_2,b_0,b_1,b_2,b_3,b_4\}^T$ and $\mathbf{v}$ is 7x1 constant vector. The expressions for the elements of matrix A for the beam under uniform axial load, gravity load and centrifugal load are given in Appendix A, Eqs. (A.3), (A.4) and (A.5), respectively. For the Rayleigh beam under an uniform axial load P, $\mathbf{v}=\{2Pc_2,6Pc_3,12Pc_4,0,0,0,0\}^T$. For the gravity-loaded and centrifugally loaded beam $\mathbf{v}=0$. Eq. (5) can be readily solved using the symbolic manipulation software MATHEMATICA. Thus, we will get the expressions for the constants a_i's and b_i's in terms of one of the unknown constant, specifically a_2. If the total mass of the beam is given by M, then the constant a_2 can be easily determined using the relation

$$\int_0^L \rho A(x)\,dx = M \tag{6}$$

The final expressions for the variation of cross-sectional area $A(x)$ and area moment of inertia $I(x)$ can be determined using Eqs. (2) and (3). From here, we can also get the mass per unit length $m(x)=\rho A(x)$ and stiffness $EI(x)$ distributions. Thus, we have used the inverse problem approach to find the beam given a solution, which in turn leads to the closed-form solution.

Thus, if an axially loaded Rayleigh beam has a cross-section area $A(x)$ and area moment of inertia $I(x)$ variations given by Eqs. (2) and (3), then the beam will vibrate with the pre-selected fundamental frequency ω, and mode shape given by Eq. (4), provided the expressions for the constants a_i's and b_i's are solved using Eq. (5). If such a beam exists it would be interesting to calculate its dimensions for practical applications. For this we consider a non-uniform Rayleigh cantilever beam with rectangular cross-section, whose height and breadth variations are given by $h(x)$ and $b(x)$, respectively. We already know $A(x)=b(x)h(x)$ and $I(x)=b(x)h(x)^3/12$. Knowing the variations of $A(x)$ and $I(x)$, the height $h(x)$ and breadth $b(x)$ can be easily calculated as

$$h(x)=\sqrt{\frac{12\,I(x)}{A(x)}},\; b(x)=\sqrt{\frac{A(x)^3}{12\,I(x)}} \tag{7}$$

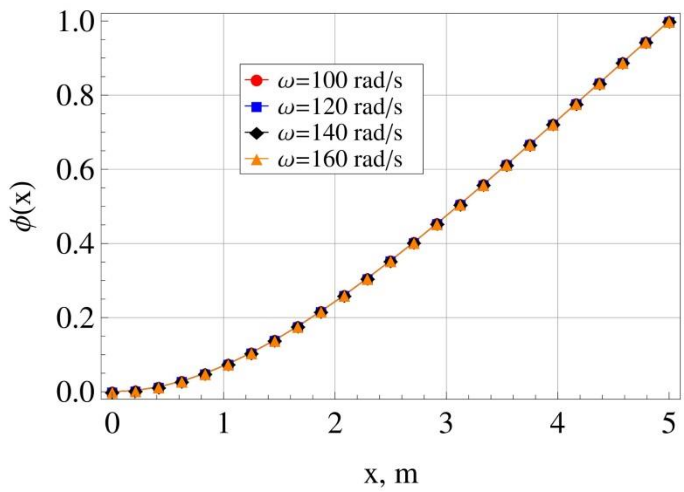

Fig. 1 The assumed mode shape $\phi(x)$ for a non-uniform Rayleigh cantilever, under uniform axial load $P = 500$ N, for different values of the assumed fundamental frequency ω

The results for the derived cross-section and area moment of inertia variations for different types of axial loading are given in the following section.

3. Results for different types of axial loading

As an example we take a non-uniform Rayleigh cantilever beam having length $L = 5$ m, material density $\rho = 7860$ kg/m^3, elastic modulus $E = 2\text{x}10^{11}$ Pa and having a total mass $M = 100$ kg. Using the procedure described in Section 2, we have derived the mass $m(x) = \rho A(x)$ and stiffness distribution $EI(x)$ for non-uniform Raleigh cantilever beam, having different types of axial loading, for a given assumed mode shape $\phi(x)$ and fundamental frequency ω. The results are given as follows:

3.1 Uniform axial load

Fig. 1 shows the assumed mode shape for a non-uniform Rayleigh cantilever beam, under a uniform axial load $P = 500$ N, for different values of the assumed fundamental frequency ω. Fig. 2 shows the mass and stiffness variations corresponding to the assumed mode shape shown in Fig. 1. The height and breadth variations for a corresponding rectangular cross-section beam are shown in Fig. 3. Thus, if a non-uniform Rayleigh cantilever beam under uniform axial load $P = 500$ N is designed according to the mass and stiffness distributions in Fig. 2, then the assumed mode shape $\phi(x)$ and fundamental frequency ω, shown in Fig. 1, will serve as exact closed-form solutions to the fourth order governing differential equation. The derived functions can thus be used for validation of numerical methods developed for the free vibration analysis of Rayleigh beams. For archival purpose, we give the polynomials expressions for the assumed mode shape $\phi(x)$, mass $m(x)$ and stiffness $EI(x)$ variations, for a non-uniform Rayleigh cantilever beam under a uniform axial load $P = 500$ N, having assumed fundamental frequency $\omega = 140$ rad/s, as follows

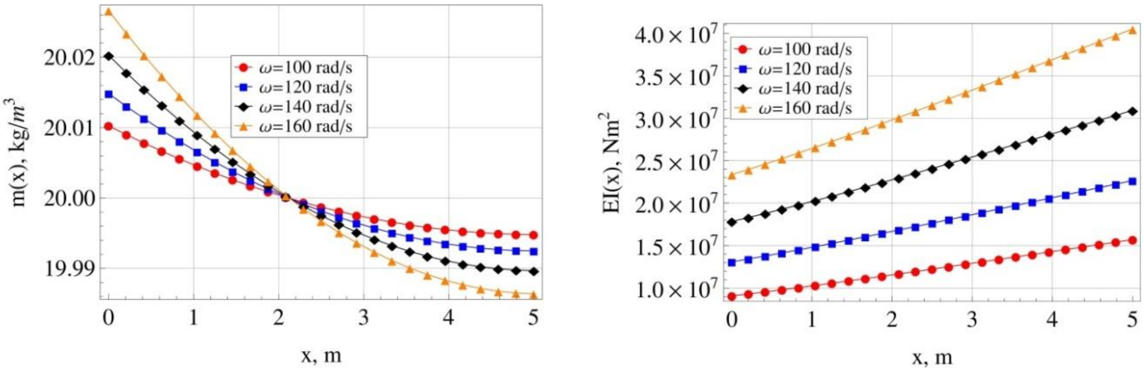

(a) (b)

Fig. 2 Property variations for a non-uniform Rayleigh cantilever, under uniform axial load $P = 500$ N, for different values of the assumed fundamental frequency ω: (a) Mass variation, (b) stiffness variation

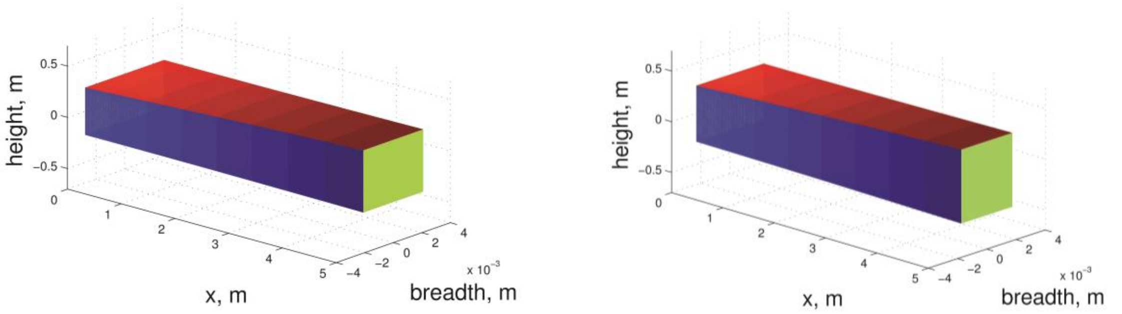

(a) For $\omega = 100$ rad/s (b) For $\omega = 120$ rad/s

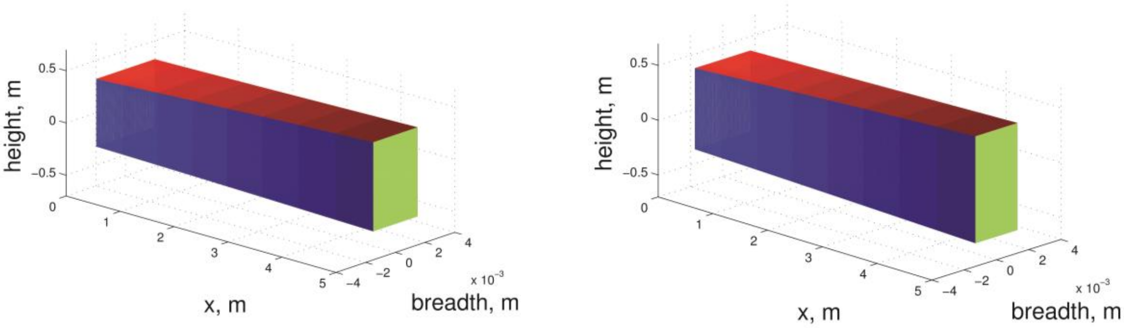

(c) For $\omega = 140$ rad/s (d) For $\omega = 160$ rad/s

Fig. 3 Height and breadth variations for a Rayleigh cantilever beam, under an uniform axial load $P = 500$ N, corresponding to the mass and stiffness variations shown in Fig. 2

$$\phi(x) = (0.0798286 - 0.0106095x + 0.000528764x^2)x^2$$
$$m(x) = 20.0203 - 0.0121087x + 0.00119767x^2$$
$$EI(x) = 1.78422\text{x}10^7 + 2.20679\text{x}10^6 x + 164160x^2 - 21937.2x^3 + 1088.4x^4 \quad (8)$$

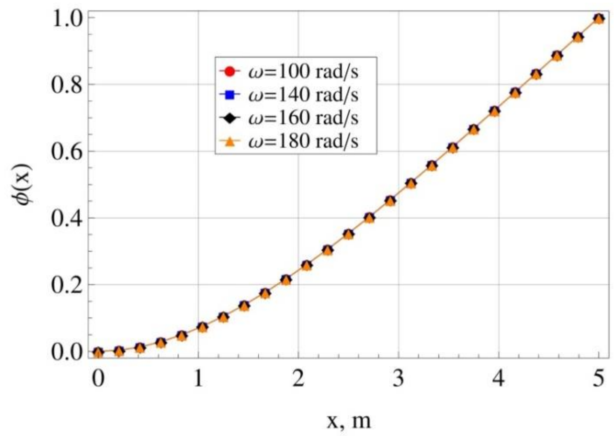

Fig. 4 The assumed mode shape $\phi(x)$ for a non-uniform gravity-loaded Rayleigh cantilever, for different values of the assumed fundamental frequency ω

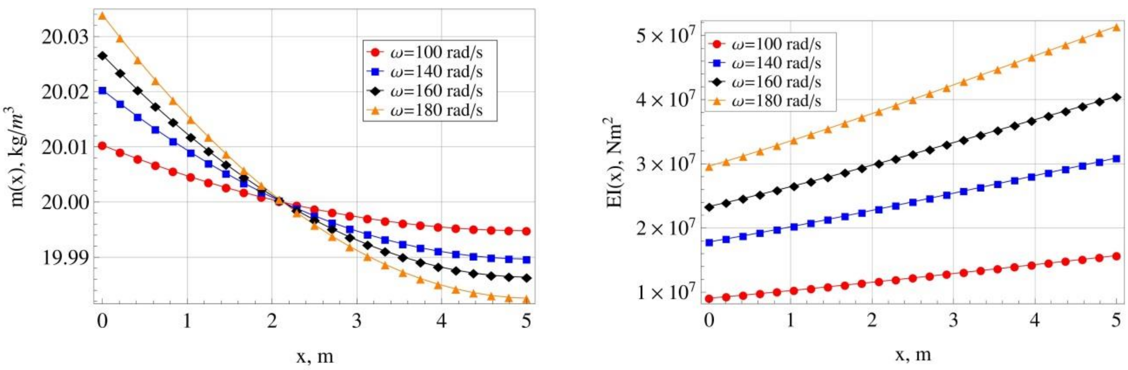

(a) (b)

Fig. 5 Property variations for a non-uniform gravity-loaded Rayleigh cantilever, for different values of the assumed fundamental frequency ω: (a) Mass variation, (b) stiffness variation

3.2 Gravity-loaded beam

Fig. 4 shows the assumed mode shapes of a non-uniform gravity-loaded Rayleigh cantilever beam, under acceleration due to gravity $g = 9.8$ m/s^2, for different values of the assumed fundamental frequency ω. Fig. 5 shows the mass and stiffness variations corresponding to the assumed mode shapes shown in Fig. 4. The height and breadth variations for a corresponding rectangular cross-section beam are shown in Fig. 6. Hence, if a non-uniform gravity-loaded Rayleigh cantilever beam is designed according to the mass and stiffness variations shown in Fig. 5, then the assumed mode shape $\phi(x)$ and fundamental frequency ω, given in Fig. 4, will serve as exact closed-form solutions to the fourth order governing differential equation. Once again, for archival purpose, we give the polynomials expressions for the assumed mode shape $\phi(x)$, mass $m(x)$ and stiffness $EI(x)$ variations, for a non-uniform gravity-loaded Rayleigh cantilever beam under acceleration due to gravity $g = 9.8$ m/s^2, having assumed fundamental frequency $\omega = 160$ rad/s, as follows

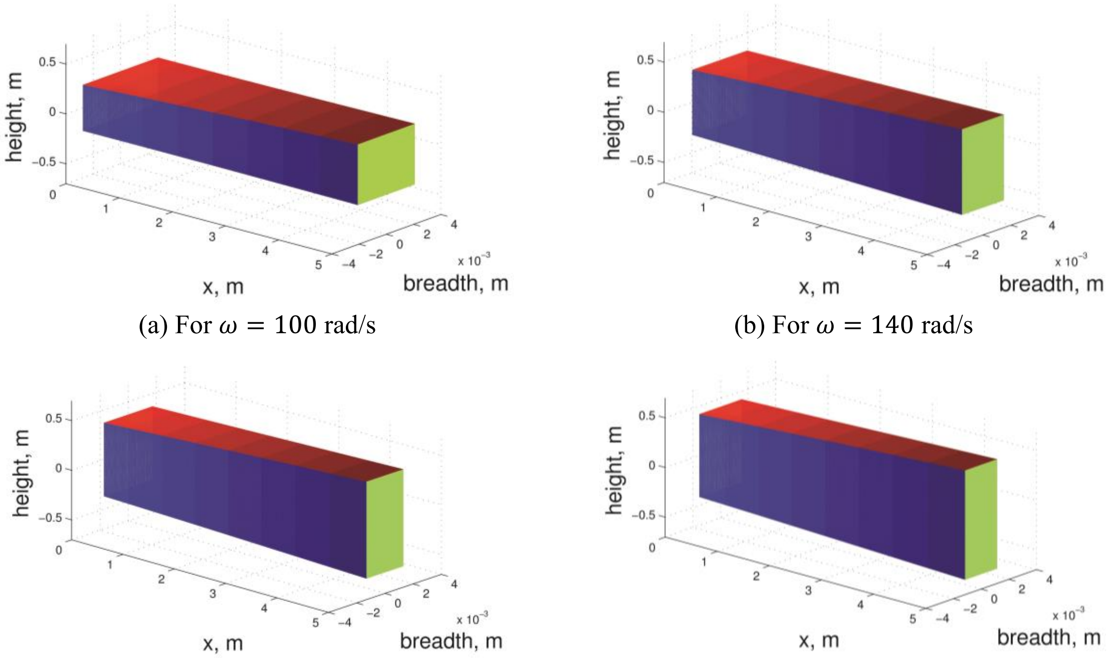

(a) For $\omega = 100$ rad/s

(b) For $\omega = 140$ rad/s

(c) For $\omega = 160$ rad/s

(d) For $\omega = 180$ rad/s

Fig. 6 Height and breadth variations for a gravity-loaded Rayleigh cantilever beam, corresponding to the mass and stiffness variations shown in Fig. 5

$$\phi(x) = (0.0797761 - 0.010592x + 0.000527363x^2)x^2$$
$$m(x) = 0.00156413(12803.7 - 10.1491x + x^2)$$
$$EI(x) = 2.33596\text{x}10^7 + 2.89381\text{x}10^6 x + 214874x^2 - 28731x^3 + 1421.42x^4 \tag{9}$$

3.3 Rotating beam

Fig. 7 shows the assumed mode shape of a non-uniform rotating Rayleigh cantilever beam, for different values of the uniform rotating speed Ω, having an assumed fundamental frequency $\omega = 140$ rad/s. Fig. 8 shows the mass and stiffness variations corresponding to the assumed mode shapes shown in Fig. 7. The height and breadth variations for a corresponding rectangular cross-section beam are shown in Fig. 9. The mass and stiffness variation shown in Fig. 8 for $\Omega = 0$ RPM corresponds to a non-rotating non-uniform Rayleigh cantilever beam. Thus, if a non-uniform Rayleigh cantilever beam is designed according to the mass and stiffness variations shown in Fig. 8, then the assumed mode shapes $\phi(x)$, shown in Fig. 7, and assumed fundamental frequency $\omega = 140$ rad/s will serve as exact closed-form solutions to the fourth order governing differential equation. For archival purpose, we give the polynomials expressions for the assumed mode shape $\phi(x)$, mass $m(x)$ and stiffness $EI(x)$ variations, for a non-uniform rotating Rayleigh cantilever beam under a uniform rotating speed $\Omega = 320$ RPM, having assumed fundamental frequency $\omega = 140$ rad/s, as follows

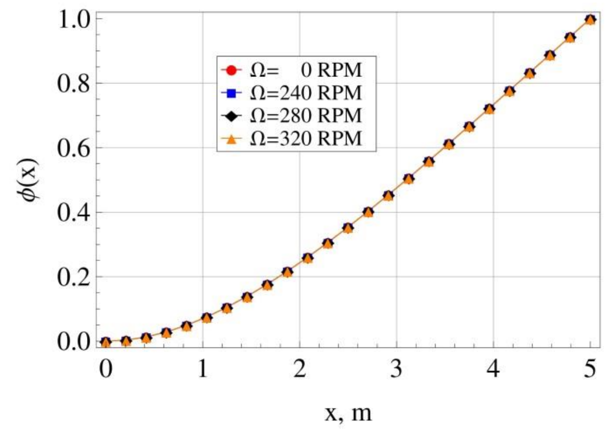

Fig. 7 The assumed mode shape $\phi(x)$ for a non-uniform rotating Rayleigh cantilever, for different values of the uniform rotating speed Ω, having an assumed fundamental frequency $\omega = 140$ rad/s

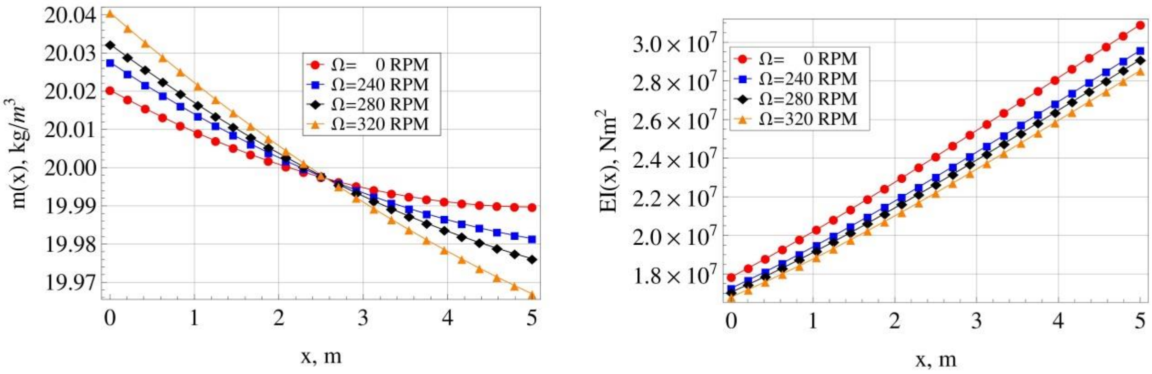

(a) (b)

Fig. 8 Property variations for a non-uniform rotating Rayleigh cantilever, for different values of the uniform rotating speed Ω, having an assumed fundamental frequency $\omega = 140$ rad/s: (a) Mass variation, (b) stiffness variation

$$
\begin{gathered}
\phi(x) = (0.0798188 - 0.0106063x + 0.000528502x^2)x^2 \\
m(x) = 20.0406 - 0.0192461x + 0.000905123x^2 \\
EI(x) = 1.68145\text{x}10^7 + 1.79854\text{x}10^6 x + 182400x^2 - 16958.9x^3 + 465.963x^4 \quad (10)
\end{gathered}
$$

4. Derived property variations used as test functions for h-FEM

The finite element method (FEM) is one of the most popular methods used for the vibration analysis of beams. Among the various methods used for the finite element method, we will use the h-version finite element method, where we use the Hermite cubic polynomials as the shape functions. In this work, we have used the inverse method to analytically derive the flexural stiffness $EI(x)$ and mass per unit $m(x)$ variations, using the governing differential equations of a axially loaded Rayleigh cantilever beam, by assuming a fundamental mode shape $\phi(x)$ and

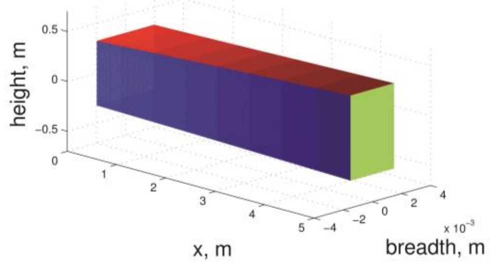

(a) For $\Omega = 0$ RPM

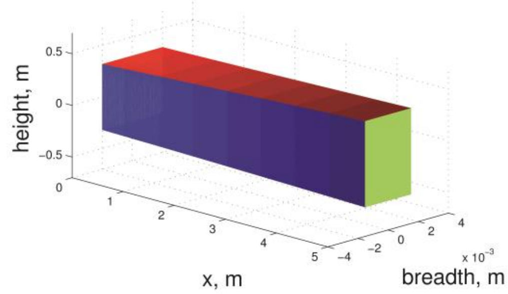

(b) For $\Omega = 240$ RPM

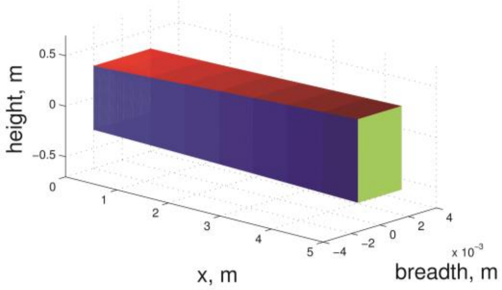

(c) For $\Omega = 280$ RPM

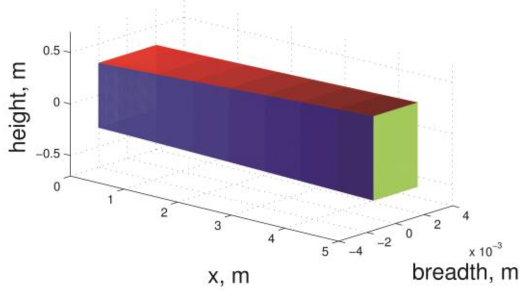

(d) For $\Omega = 320$ RPM

Fig. 9 Height and breadth variations for a rotating Rayleigh cantilever beam, corresponding to the mass and stiffness variations shown in Fig. 8

Table 3 Comparison of the assumed fundamental frequencies and the ones derived numerically using the h-FEM

Axial loading type	Load value	Assumed fundamental frequency (rad/s)	h-FEM fundamental frequency (rad/s)
Uniform axial load	$P = 500$ N	100	100.026
		120	120.022
		140	140.018
		160	160.016
Gravity-loaded	$g = 9.8$ m/s^2	100	100.00
		140	140.00
		160	160.00
		180	180.00
Centrifugally-loaded	Ω=0 RPM	140	140.00
	Ω = 240 RPM	140	140.001
	Ω = 280 RPM	140	140.002
	Ω = 320 RPM	140	140.004

frequency ω. So theoretically, if we were to put the derived mass and stiffness variations into a numerical code like the finite element method, we would get back the assumed fundamental mode shape and frequency numerically. We used the derived mass and stiffness variations shown in Figs. 2, 5 and 8, and put them into the h-FEM code. We used 200 uniform elements to discretize the beam, and the results obtained for the different axial loading types are shown in Table 3. Hence,

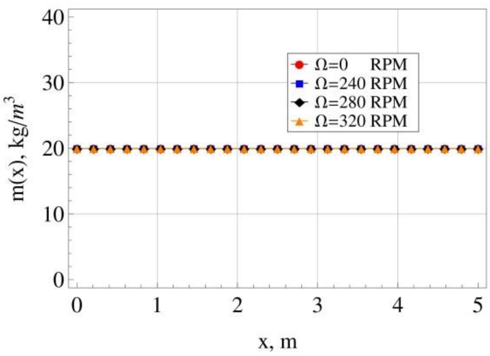

(a)

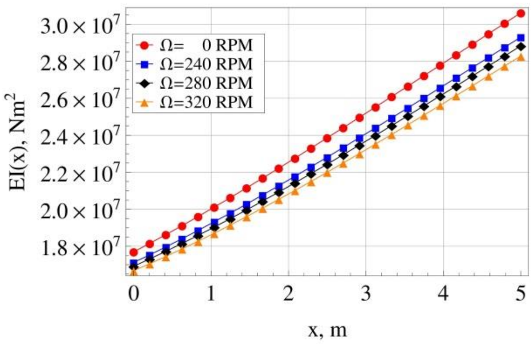

(b)

Fig. 10 Property variations for a non-uniform rotating Euler-Bernoulli cantilever beam, for different values of the uniform rotating speed Ω, having an assumed fundamental frequency $\omega = 140$ rad/s: (a) Mass variation, (b) stiffness variation

showing the usefulness of the derived property variations as test functions for different numerical methods which are routinely developed by researchers to study the free vibration of Rayleigh beams.

5. Comparison with Euler-Bernoulli beam theory

As a comparison, we can use the same beam properties, boundary condition, assumed frequency and uniform rotation speed to derive the mass and stiffness variations of the rotating beam using the Euler-Bernoulli beam theory (EBT). A detailed account of the study can found in the work by (Sarkar and Ganguli 2014b). The derived mass and stiffness variations for a rotating cantilever Euler-Bernoulli beam are shown in Fig. 10. As expected, the mass variation turns out to be constant, because the stiffness variation was assumed to be a fourth order polynomial. This is because for the inverse problem derivation using EBT, the difference in the polynomial order between the stiffness and mass variations should be four (Sarkar and Ganguli 2014b). For a more comparative angle, we have shown the height and breadth variations for the rectangular cross-section rotating cantilever Rayleigh and Euler-Bernoulli beam, having assumed fundamental frequency $\omega = 140$ rad/s and uniform rotation speed of $\Omega = 320$ RPM, in Fig. 11. From Fig. 11, we can see that the difference in the dimensions of the rectangular cross-section beams derived using the Rayleigh and Euler-Bernoulli beam are very similar. This can be attributed to the fact that in our example we took a long and slender beam, which is very well modeled by the EBT. Hence, using a higher order beam theory, namely the Rayleigh beam theory (RBT), the results does not differ significantly for this particular example.

But, for short and thick beams, the RBT predicts the frequencies and mode shapes more accurately as compared to the EBT, especially for high frequency vibration. In order to meet the above mentioned criteria, we have considered another numerical example with the following values for the various parameters: length $L = 1$m, assumed frequency $\omega = 2000$ rad/s, uniform rotation speed $\Omega = 2000$ RPM and total mass $M_{tot} = 1000$ kg. Using these values, we derived the mass and stiffness variations using both RBT and EBT. Fig. 12 shows the corresponding height

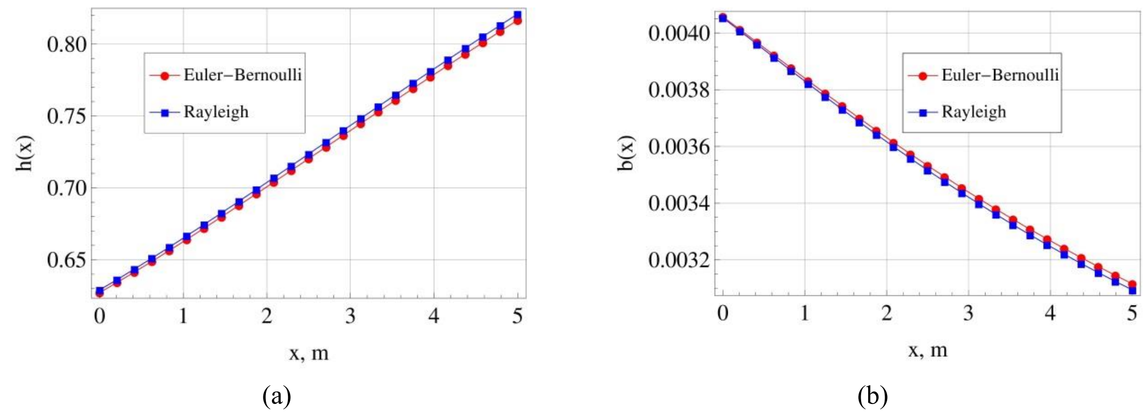

Fig. 11 Comparing the dimensions of a rectangular cross-section rotating cantilever Rayleigh and Euler-Bernoulli beam, for $L = 5$m, $\omega = 140$ rad/s, $\Omega = 320$ RPM and $M_{tot} = 100$ kg: (a) Height variation, (b) breadth variation

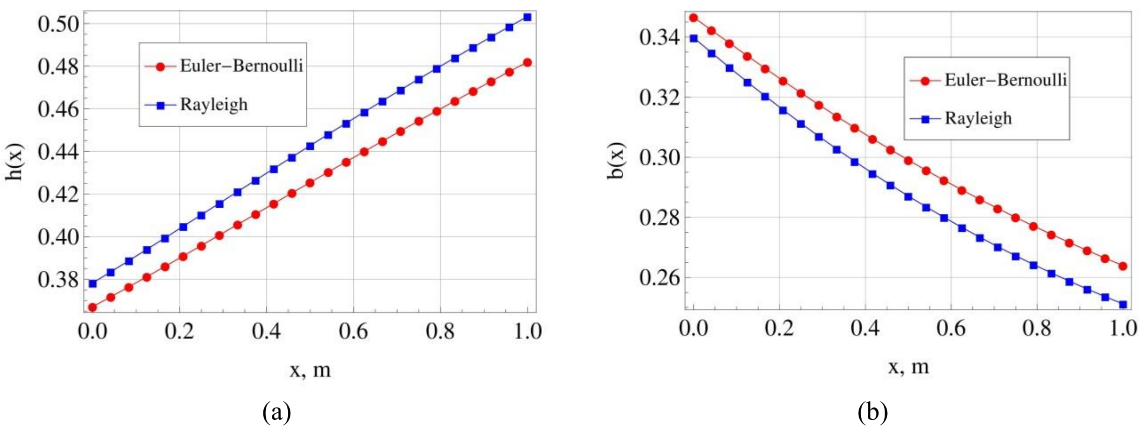

Fig. 12 Comparing the dimensions of a rectangular cross-section rotating cantilever Rayleigh and Euler-Bernoulli beam, for $L = 1$m, $\omega = 1000$ rad/s, $\Omega = 2000$ RPM and $M_{tot} = 1000$ kg: (a) Height variation, (b) breadth variation

and breadth variations for a rectangular cross-section cantilever Rayleigh and Euler-Bernoulli beam, having assumed fundamental frequency $\omega = 2000$ rad/s and uniform rotation speed $\Omega = 2000$ RPM. From Fig. 12, we observe that there is a significant difference (around 10~20 mm) between the dimensions of the rotating beams derived using RBT and EBT. Since, the height and breadth variations in Fig. 12 are of the same order, we can deduce that the area moment of inertia variation $I(x)$ $(= b(x)h(x)^3/12)$ will be less for the Euler-Bernoulli beam as compared to the Rayleigh beam, whereas the cross-section variation $A(x)$ $(= b(x)h(x))$ is comparable. Hence, the stiffness variation $EI(x)$ is higher for the rotating Rayleigh beam as compared the Euler-Bernoulli beam, although both of them have the same assumed fundamental frequency ω. This is a classic example of the fact that for short and thick beams and high frequency vibration, the EBT over predicts the frequency.

4. Conclusions

In this paper, we have shown that there exists a certain class of non-uniform Rayleigh cantilever beam, under uniform, gravity-loaded and centrifugal type of axial loading, which has a closed form polynomial solution to its governing differential equation. We assume a certain mode shape function $\phi(x)$, which satisfies all the given boundary conditions, from which we derived the mass distribution $m(x)$ and flexural stiffness $EI(x)$ of the beam. These derived properties are simple polynomial functions which depend on the fundamental frequency ω, length of the beam L, the material density ρ, elastic modulus E and the type of axial loading. So essentially, given a certain fundamental frequency ω, we can tailor the properties of the non-uniform Rayleigh beam. This might be useful for some practical design applications where the fundamental frequency might be required to assume a desired value. But most importantly, these closed-form solutions serve as benchmark solutions for the validation of numerical or approximate methods used for non-uniform Rayleigh beam vibration analysis under different types of axial loading. For the case of the rotating cantilever beam, the results derived using Rayleigh theory were also compared with those derived using the Euler-Bernoulli beam theory.

Reasonable question arises why not to deal with Timoshenko beams, rather than with the Rayleigh beams. In fact, it is well known that the Timoshenko beam theory incorporates the rotary inertia and shear deformation, and thus is more accurate than the Rayleigh beam theory. It was felt, that the closed-form solutions within the Rayleigh theory provide improvements over the Euler-Bernoulli theory without getting into the complicated coupled governing differential equation of a Timoshenko beam, as well as some guide into the behaviour of the Timoshenko beams. Indeed, the same consideration apparently led authors of references (Banerjee and Jackson 2013, Chang, Lin *et al.* 2010, Li, Tang *et al.* 2013, Pai, Qian *et al.* 2013, Stojanović and Kozić 2012, Xi, Li *et al.* 2013) to study the Rayleigh beams. Closest analogue to the Rayleigh beam appears to be an Euler-Bernoulli beam with tip mass of considerable size so that its rotary inertia has a significant effect. Study of beams with a concentrated mass is underway and will be reported elsewhere.

References

Abedinnasab, M.H., Zohoor, H. and Yoon, Y.J. (2012), "Exact formulations of non-linear planar and spatial Euler-Bernoulli beams with finite strains", *P. I. Mech. Eng. C - J. Mech. Eng. Sci*., **226**(5), 1225-1236.

Auciello, N. and Lippiello, M. (2013), "Vibration analysis of rotating non-uniform Rayleigh beams using "CDM" method", *Global Virtual Conference*.

Aydin, K. (2013), "Influence of Crack and Slenderness Ratio on the Eigenfrequencies of Euler-Bernoulli and Timoshenko Beams", *Mech. Adv. Mater. Struct*., **20**(5), 339-352.

Bağdatlı, S.M. and Uslu, B. (2015), "Free vibration analysis of axially moving beam under non-ideal conditions", *Struct. Eng. Mech*., **54**(3), 597-605.

Baghani, M., Mohammadi, H. and Naghdabadi, R. (2014), "An analytical solution for shape-memory-polymer Euler-Bernoulli beams under bending", *Int. J. Mech. Sci.*, **84**, 84-90.

Bambill, D., Rossit, C., Rossi, R., Felix, D. and Ratazzi, A. (2013), "Transverse free vibration of non uniform rotating Timoshenko beams with elastically clamped boundary conditions", *Meccanica*, **48**(6), 1289-1311.

Banerjee, J. R. and Jackson, D. (2013), "Free vibration of a rotating tapered Rayleigh beam: a dynamic stiffness method of solution", *Comput. Struct*., **124**, 11-20.

Calim, F.F. (2016), "Dynamic response of curved Timoshenko beams resting on viscoelastic foundation",

Struct. Eng. Mech., **59**(4), 761-774.
Chang, J.R., Lin, W.J., Huang, C.J. and Choi, S.T. (2010), "Vibration and stability of an axially moving Rayleigh beam", *Appl. Math. Model.*, **34**(6), 1482-1497.
Datta, P. and Ganguli, R. (1990), "Vibration characteristics of a rotating blade with localized damage including the effects of shear deformation and rotary inertia", *Comput. Struct.*, **36**(6), 1129-1133.
Ebrahimi, F. and Jafari, A. (2016), "Thermo-mechanical vibration analysis of temperature dependent porous FG beams based on Timoshenko beam theory", *Struct. Eng. Mech.*, **59**(2), 343-371.
Elishakoff, I. (2004), *Eigenvalues Of Inhomogeneous Structures: Unusual Closed-form Solutions*: CRC Press, Boca Raton, Florida, USA.
Elishakoff, I. and Guede, Z. (2004), "Analytical polynomial solutions for vibrating axially graded beams", *Mech. Adv. Mater. Struct.*, **11**(6), 517-533.
Gunda, J.B. and Ganguli, R. (2008), "Stiff-string basis functions for vibration analysis of high speed rotating beams", *J. Appl. Mech.*, **75**(2), 024502.
Ke, L.L., Yang, J., Kitipornchai, S. and Xiang, Y. (2009), "Flexural vibration and elastic buckling of a cracked Timoshenko beam made of functionally graded materials", *Mech. Adv. Mater. Struct.*, **16**(6), 488-502.
Li, X., Tang, A. and Xi, L. (2013), "Vibration of a Rayleigh cantilever beam with axial force and tip mass", *J. Constr. Steel Res.*, **80**, 15-22.
Liu, Z., Yin, Y., Wang, F., Zhao, Y. and Cai, L. (2013), "Study on modified differential transform method for free vibration analysis of uniform Euler-Bernoulli beam", *Struct. Eng. Mech.*, **48**(5), 697-709.
Lou, P., Dai, G. and Zeng, Q. (2006), "Finite-element analysis for a Timoshenko beam subjected to a moving mass", *P. I. Mech. Eng. C - J. Mech. Eng. Sci.*, **220**(5), 669-678.
Ma'en, S.S. and Butcher, E.A. (2012), "Free vibration analysis of non-rotating and rotating Timoshenko beams with damaged boundaries using the Chebyshev collocation method", *Int. J. Mech. Sci.*, **60**(1), 1-11.
Maiz, S., Bambill, D.V., Rossit, C.A. and Laura, P. (2007), "Transverse vibration of Bernoulli-Euler beams carrying point masses and taking into account their rotatory inertia: exact solution", *J. Sound Vib.*, **303**(3), 895-908.
Mao, Q. (2015), "AMDM for free vibration analysis of rotating tapered beams", *Struct. Eng. Mech.*, **54**(3), 419-432.
Pai, P.F., Qian, X. and Du, X. (2013), "Modeling and dynamic characteristics of spinning Rayleigh beams", *Int. J. Mech. Sci.*, **68**, 291-303.
Sarkar, K. (2012), "Closed-Form Solutions for Rotating and Non-Rotating Beams: An Inverse Problem Approach", M.Sc (Engg) Thesis.
Sarkar, K. and Ganguli, R. (2013), "Closed-form solutions for non-uniform Euler-Bernoulli free-free beams", *J. Sound Vib.*, **332**(23), 6078-6092.
Sarkar, K. and Ganguli, R. (2014a), "Analytical test functions for free vibration analysis of rotating non-homogeneous Timoshenko beams", *Meccanica*, **49**(6), 1469-1477.
Sarkar, K. and Ganguli, R. (2014b), "Modal tailoring and closed-form solutions for rotating non-uniform Euler-Bernoulli beams", *Int. J. Mech. Sci.*, **88**, 208-220.
Sarkar, K. and Ganguli, R. (2014c), "Tailoring the second mode of Euler-Bernoulli beams: an analytical approach", *Struct. Eng. Mech.*, **51**(5), 773-792.
Shahba, A., Attarnejad, R. and Hajilar, S. (2011), "Free vibration and stability of axially functionally graded tapered Euler-Bernoulli beams", *Shock Vib.*, **18**(5), 683-696.
Stojanović, V. and Kozić, P. (2012), "Forced transverse vibration of Rayleigh and Timoshenko double-beam system with effect of compressive axial load", *Int. J. Mech. Sci.*, **60**(1), 59-71.
Tang, A.Y., Li, X.F., Wu, J.X. and Lee, K. (2015), "Flapwise bending vibration of rotating tapered Rayleigh cantilever beams", *J. Constr. Steel Res.*, **112**, 1-9.
Tang, A.Y., Wu, J.X., Li, X.F. and Lee, K. (2014), "Exact frequency equations of free vibration of exponentially non-uniform functionally graded Timoshenko beams", *Int. J. Mech. Sci.*, **89**, 1-11.
Xi, L.Y., Li, X.F. and Tang, G.J. (2013), "Free vibration of standing and hanging gravity-loaded Rayleigh cantilevers", *Int. J. Mech. Sci.*, **66**, 233-238.

Yesilce, Y. (2015), "Differential transform method and numerical assembly technique for free vibration analysis of the axial-loaded Timoshenko multiple-step beam carrying a number of intermediate lumped masses and rotary inertias", *Struct. Eng. Mech.*, **53**(3), 537-573.

Zahrai, S.M., Mortezagholi, M.H. and Mirsalehi, M. (2016), "Effect of higher order terms of Maclaurin expansion in nonlinear analysis of the Bernoulli beam by single finite element", *Struct. Eng. Mech.*, **58**(6), 949-966.

CC

Appendix. A. Expressions for the constants c_i's, matrices $\mathbf{A}$'s and vectors $\mathbf{v}$'s

The expressions for the constants c_i's in the Eq. (4), for the Rayleigh beam under uniform axial load and gravity load is given by

$$c_0 = 0, c_1 = 0, c_2 = \frac{6(\alpha L^2\omega^2 - 6)}{L^2(\alpha L^2\omega^2 - 18)}, c_3 = -\frac{8(\alpha L^2\omega^2 - 3)}{L^3(\alpha L^2\omega^2 - 18)}, c_4 = \frac{3(\alpha L^2\omega^2 - 2)}{L^4(\alpha L^2\omega^2 - 18)} \quad (A.1)$$

The expressions for the constants c_i's in the Eq. (4), for the Rayleigh beam under centrifugal load is given by

$$c_0 = 0, c_1 = 0, c_2 = \frac{6(\alpha L^2(\omega^2 + \Omega^2) - 6)}{L^2(\alpha L^2(\omega^2 + \Omega^2) - 18)}, c_3 = -\frac{8(\alpha L^2(\omega^2 + \Omega^2) - 3)}{L^3(\alpha L^2(\omega^2 + \Omega^2) - 18)},$$
$$c_4 = \frac{3(\alpha L^2(\omega^2 + \Omega^2) - 2)}{L^4(\alpha L^2(\omega^2 + \Omega^2) - 18)} \quad (A.2)$$

The expression for the matrix **A** for the Rayleigh beam under uniform axial loading, gravity loading and centrifugal loading are given by

$$\mathbf{A} = \begin{pmatrix} -\rho\omega^2 c_0 & 0 & 0 & 2\rho c_2\omega^2 + 24Ec_4 & \rho c_1\omega^2 + 12Ec_3 & 4Ec_2 & 0 & 0 \\ -\rho\omega^2 c_1 & -\rho\omega^2 c_0 & 0 & 6\rho\omega^2 c_3 & 4\rho c_2\omega^2 + 72Ec_4 & 2\rho c_1\omega^2 + 36Ec_3 & 12Ec_2 & 0 \\ -\rho\omega^2 c_2 & -\rho\omega^2 c_1 & -\rho\omega^2 c_0 & 12\rho\omega^2 c_4 & 9\rho\omega^2 c_3 & 6\rho c_2\omega^2 + 144Ec_4 & 3\rho c_1\omega^2 + 72Ec_3 & 24Ec_2 \\ -\rho\omega^2 c_3 & -\rho\omega^2 c_2 & -\rho\omega^2 c_1 & 0 & 16\rho\omega^2 c_4 & 12\rho\omega^2 c_3 & 8\rho c_2\omega^2 + 240Ec_4 & 4\rho c_1\omega^2 + 120Ec_3 \\ -\rho\omega^2 c_4 & -\rho\omega^2 c_3 & -\rho\omega^2 c_2 & 0 & 0 & 20\rho\omega^2 c_4 & 15\rho\omega^2 c_3 & 10\rho c_2\omega^2 + 360Ec_4 \\ 0 & -\rho\omega^2 c_4 & -\rho\omega^2 c_3 & 0 & 0 & 0 & 24\rho\omega^2 c_4 & 18\rho\omega^2 c_3 \\ 0 & 0 & -\rho\omega^2 c_4 & 0 & 0 & 0 & 0 & 28\rho\omega^2 c_4 \end{pmatrix} \tag{A.3}$$

$$\mathbf{A} = \begin{pmatrix} -\rho c_0\omega^2 + g\rho c_1 - 2gL\rho c_2 & -gL^2\rho c_2 & \frac{1}{3}(-2)gL^3\rho c_2 & 2\rho c_2\omega^2 + 24Ec_4 & \rho c_1\omega^2 + 12Ec_3 & 4Ec_2 & 0 & 0 \\ -\rho c_1\omega^2 + 4g\rho c_2 - 6gL\rho c_3 & -3g\rho c_3 L^2 - \rho\omega^2 c_0 + g\rho c_1 & -2gL^3\rho c_3 & 6\rho\omega^2 c_3 & 4\rho c_2\omega^2 + 72Ec_4 & 2\rho c_1\omega^2 + 36Ec_3 & 12Ec_2 & 0 \\ -\rho c_2\omega^2 + 9g\rho c_3 - 12gL\rho c_4 & -6g\rho c_4 L^2 - \rho\omega^2 c_1 + 3g\rho c_2 & -4g\rho c_4 L^3 - \rho\omega^2 c_0 + g\rho c_1 & 12\rho\omega^2 c_4 & 9\rho\omega^2 c_3 & 6\rho c_2\omega^2 + 144Ec_4 & 3\rho c_1\omega^2 + 72Ec_3 & 24Ec_2 \\ 16g\rho c_4 - \rho\omega^2 c_3 & 6g\rho c_3 - \rho\omega^2 c_2 & \frac{8}{3}g\rho c_2 - \rho\omega^2 c_1 & 0 & 16\rho\omega^2 c_4 & 12\rho\omega^2 c_3 & 8\rho c_2\omega^2 + 240Ec_4 & 4\rho c_1\omega^2 + 120Ec_3 \\ -\rho\omega^2 c_4 & 10g\rho c_4 - \rho\omega^2 c_3 & 5g\rho c_3 - \rho\omega^2 c_2 & 0 & 0 & 20\rho\omega^2 c_4 & 15\rho\omega^2 c_3 & 10\rho c_2\omega^2 + 360Ec_4 \\ 0 & -\rho\omega^2 c_4 & 8g\rho c_4 - \rho\omega^2 c_3 & 0 & 0 & 0 & 24\rho\omega^2 c_4 & 18\rho\omega^2 c_3 \\ 0 & 0 & -\rho\omega^2 c_4 & 0 & 0 & 0 & 0 & 28\rho\omega^2 c_4 \end{pmatrix} \tag{A.4}$$

$$\mathbf{A} = \left| \begin{matrix} -\rho c_0\omega^2 - L^2\rho\Omega^2 c_2 & \frac{1}{3}(-2)L^3\rho\Omega^2 c_2 & -\frac{1}{2}L^4\rho\Omega^2 c_2 & 2\rho c_2\omega^2 + 2\rho\Omega^2 c_2 + 24Ec_4 & \rho c_1\omega^2 + \rho\Omega^2 c_1 + 12Ec_3 & 4Ec_2 & 0 & 0 \\ -\rho c_1\omega^2 + \rho\Omega^2 c_1 - 3L^2\rho\Omega^2 c_3 & -2\rho\Omega^2 c_3 L^3 - \rho\omega^2 c_0 & \frac{1}{2}(-3)L^4\rho\Omega^2 c_3 & 6\rho c_3\omega^2 + 6\rho\Omega^2 c_3 & 4\rho c_2\omega^2 + 4\rho\Omega^2 c_2 + 72Ec_4 & 2\rho c_1\omega^2 + 2\rho\Omega^2 c_1 + 36Ec_3 & 12Ec_2 & 0 \\ -\rho c_2\omega^2 + 3\rho\Omega^2 c_2 - 6L^2\rho\Omega^2 c_4 & -4\rho\Omega^2 c_4 L^3 - \rho\omega^2 c_1 + \rho\Omega^2 c_1 & -3\rho\Omega^2 c_4 L^4 - \rho\omega^2 c_0 & 12\rho c_4\omega^2 + 12\rho\Omega^2 c_4 & 9\rho c_3\omega^2 + 9\rho\Omega^2 c_3 & 6\rho c_2\omega^2 + 6\rho\Omega^2 c_2 + 144Ec_4 & 3\rho c_1\omega^2 + 3\rho\Omega^2 c_1 + 72Ec_3 & 24Ec_2 \\ 6\rho\Omega^2 c_3 - \rho\omega^2 c_3 & \frac{8}{3}\rho\Omega^2 c_2 - \rho\omega^2 c_2 & \rho\Omega^2 c_1 - \rho\omega^2 c_1 & 0 & 16\rho c_4\omega^2 + 16\rho\Omega^2 c_4 & 12\rho c_3\omega^2 + 12\rho\Omega^2 c_3 & 8\rho c_2\omega^2 + 8\rho\Omega^2 c_2 + 240Ec_4 & 4\rho c_1\omega^2 + 4\rho\Omega^2 c_1 + 120Ec_3 \\ 10\rho\Omega^2 c_4 - \rho\omega^2 c_4 & 5\rho\Omega^2 c_3 - \rho\omega^2 c_3 & \frac{5}{2}\rho\Omega^2 c_2 - \rho\omega^2 c_2 & 0 & 0 & 20\rho c_4\omega^2 + 20\rho\Omega^2 c_4 & 15\rho c_3\omega^2 + 15\rho\Omega^2 c_3 & 10\rho c_2\omega^2 + 10\rho\Omega^2 c_2 + 360Ec_4 \\ 0 & 8\rho\Omega^2 c_4 - \rho\omega^2 c_4 & \frac{9}{2}\rho\Omega^2 c_3 - \rho\omega^2 c_3 & 0 & 0 & 0 & 24\rho c_4\omega^2 + 24\rho\Omega^2 c_4 & 18\rho c_3\omega^2 + 18\rho\Omega^2 c_3 \\ 0 & 0 & 7\rho\Omega^2 c_4 - \rho\omega^2 c_4 & 0 & 0 & 0 & 0 & 28\rho c_4\omega^2 + 28\rho\Omega^2 c_4 \end{matrix} \right| \tag{A.5}$$